JMEPEG (2006) 15:525-534
DOI: 10.1361/105994906X136098

1059-9495/$19.00

Improving Tribological Properties and Machining Performance of a-C Coatings by Doping with Titanium

W.H. Kao, Y.L. Su, and S.H. Yao

(Submitted October 10, 2005)

In this study, a-C:Ti$_{x\%}$ coatings with various levels of Ti addition are deposited on cemented tungsten carbide (WC-Co) substrates using a medium-frequency twin magnetron sputtering and unbalanced magnetron sputtering system. This study investigates the tribological properties of the coatings by conducting wear tests against an AISI 1045 steel counterbody under a cylinder-on-disk line contact wear mode using an oscillating friction and wear tester. Additionally, turning tests and high-speed through-hole drilling tests are performed on AISI 1045 steel counterbodies and PCB workpieces, respectively, to investigate the machining performance of coated turning cutters and microdrills. The a-C:Ti$_{x\%}$ coatings not only have improved tribological properties but also demonstrate enhanced machining performance. For sliding against the AISI 1045 steel counterbody under loads of 10 and 100 N, the results show that the optimal friction and wear resistance properties are provided by the a-C:Ti$_{13\%}$ and a-C:Ti$_{3\%}$ coatings, respectively. Meanwhile, the a-C:Ti$_{20\%}$ and a-C:Ti$_{51\%}$ coatings yield the optimal turning and drilling performance, respectively.

Keywords a-C:Ti$_{x\%}$ coating, machining performance, tribological properties

1. Introduction

Amorphous carbon (also known as diamond-like carbon or DLC) can be classified as either hydrogen-free amorphous carbon (a-C) or hydrogenated amorphous carbon (a-C:H). DLC is an ideal surface coating material because it possesses high hardness, good chemical resistance, and excellent tribological properties (Ref 1-13). a-C films have attracted considerable attention in the tribological and semiconductor fields because they possess exceptional properties, including good corrosion resistance, high wear resistance, low friction characteristics, high hardness, high electrical resistivity, high thermal conductivity, high dielectric strength, and good infrared (IR) optical transparency. The favorable properties of a-C coatings have led to their widespread application throughout the engineering, electronic, optical, and biological fields (Ref 14-17). Many researchers have investigated the basic physical, mechanical, and tribological properties of a-C and have attempted to further improve its adhesive and tribological properties by developing so-called a-C:Me films, in which the a-C film is doped with additional metal materials (Ref 18-22). The tribological behavior of a-C:Me coatings is dependent on their composition and structure. The a-C:Me coating that provides the optimal performance in one particular application is not necessarily the most appropriate coating for another application. Therefore, it is essential that the tribological behavior of a-C:Me coatings under different operating conditions be fully understood.

Using a medium-frequency twin magnetron sputtering and unbalanced magnetron sputtering system, this study deposits a-C:Ti$_{x\%}$ coatings with various levels of Ti addition on cemented tungsten carbide (WC-Co) disks, turning cutters, and microdrills. The coated turning cutters are tested against AISI 1045 steel counterbodies and the microdrills used in the high-speed through-drilling of printed circuit board (PCB) workpieces to establish the optimal a-C:Ti$_{x\%}$ coating for each application.

W.H. Kao, Institute of Mechatronoptic Systems, Chienkuo Technology University, Changhua, Taiwan; **Y.L. Su,** Department of Mechanical Engineering, National Cheng Kung University, Tainan, Taiwan; and **S.H. Yao,** Department of Accounting & Informing System, Chang Jung Christian University, Tainan, Taiwan. Contact e-mail: n18851158@yahoo.com.tw.

2. Experimental Details

2.1 Specimen Preparation

The cylinders used as the upper specimens (counterbodies) in the wear tester were AISI 1045 steel (H_v 286, 50 g), cut off directly from round as-purchased stock and then mechanically polished to a roughness of $R_a \approx 0.32$ μm. Meanwhile, the lower specimens, used as the coating substrates, were cemented WC-Co disks, whose surfaces were mechanically polished to $R_a \approx 0.008$ μm. After machining the disk and cylinder specimens to the exact dimensions required to fit the wear tester apparatus, the specimens were ultrasonically cleaned in acetone and then stored in an electric dryer to protect their surfaces from recontamination.

2.2 Tribology Tests

The tribological properties of the various coatings were evaluated using a Schwingung Reibung Verschleiß (SRV) oscillation friction and wear tester (Optimol Instruments Prüftechnik GmbH, Munich, Germany). Figure 1 presents a schematic diagram of the experimental setup and indicates the dimensions of the upper and lower test specimens. The arrangement of a cylinder mating with a disk forms the cylinder-on-disk line contact wear mode. The wear tests were performed at room temperature under atmospheric pressure. The relative

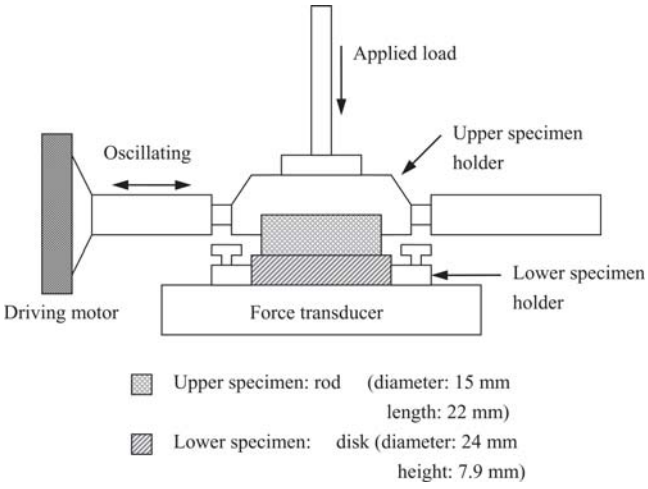

Fig. 1 SRV wear test machine

humidity of the laboratory was ~45-55%. Each coating was wear tested for 24 min. For each coating, two wear tests were performed, using new disks and cylinders in each test. After each wear test, the maximum depth of the wear scars on the lower disk was established using a surface profilometer (Surfcorder SE-30H, Kosaka Laboratory Ltd, Tokyo, Japan) with a precision of ±0.05 μm at a magnification of 2×10^4. Three depth measurements were taken from each tested disk. A total of six maximum wear depth measurements obtained for each coating were then averaged to give an overall wear depth for the coating.

2.3 Machining Tests

2.3.1 Turning Test. In the turning tests, an indexable WC turning cutter (catalog No. TNMA160404 Hti10, Mitsubishi, Japan) of grade ISO K10 was used to machine AISI 1045 bar steel. The turning cutter had a triangular geometry with sides of 12 mm and a thickness of 5 mm. The machining performance of the turning cutter was evaluated by measuring the flank wear on the cutting edge. The turning tests were performed on a traditional lathe (catalog No. TSW-70K, TaShi, Taiwan) under the following operating conditions: rotation speed, 275 rpm; depth of cut, 2.0 mm; feed rate, 0.066 mm/rev; and duration, 27.5 min. Two turning tests were performed for each coated cutter, and three flank wear measurements were obtained in each test. The overall flank wear measurement for each coated cutter was taken as the average of the six individual flank wear measurements.

2.3.2 Drilling Test. To investigate the feasibility of applying the coatings to industrial machining applications, the coatings showing better wear resistance in the turning tests were deposited on microdrills and used in a series of drilling tests. Using a commercial machining center (Prosys1, Anderson, Taiwan), high-speed through-hole drilling tests were performed on PCB substrates to assess the machining performance of the various coated microdrills. The drilling tests were performed using WC microdrills (RH-RDS, Tungaloy, Taiwan) with the following geometrical configuration: diameter, 0.3 mm; overall length, 38.1 mm; fluted length, 5.4 mm; helix angle, 35°; and point angle, 135°. The PCB boards measured 120 × 120 × 1.6 mm and were formed of glass fibers embedded in epoxy resin. The boards were coated on either side with a copper layer 35 μm thick. Drilling was performed at a rotation speed of 100,000 rpm and a feed rate of 6.8 m/min.

For each coating, five microdrills were prepared and tested. Machining performance of each coated microdrill was evaluated with an optical measurement system to measure the corner wear of the cutting edge after the drilling of 1000, 5000, 10,000, 15,000, and 20,000 holes, respectively, under dry conditions. The wear value of each coating was then established by calculating the average of the five individual wear test measurements.

2.4 Coating Deposition

The present coatings were deposited using the Genco Twinlab system (GENCOA Ltd., Liverpool, UK). This system comprised a medium-frequency twin balanced magnetron sputtering system and an unbalanced magnetron sputtering system. Each system had two targets, namely, titanium and carbon targets in the unbalanced magnetron sputtering system and two carbon targets in the balanced magnetron system. Prior to deposition, the substrates were sputter-cleaned by Ar^+ bombardment for 10 min at a bias of −350 V. A 0.1 μm Ti interlayer was then deposited on each substrate to improve the adhesion of the coatings. During the deposition process, both systems were operated simultaneously and the balanced magnetron sputtering system was connected to an oscillator to generate a magnetic field alternating at a medium frequency of 800 Hz. The distance between the substrates and the targets was 10 cm. The percentage addition of Ti metal in each a:C-$Ti_{x\%}$ coating was varied by adjusting the magnitude of the current applied to the Ti target. The coatings were all grown for the same deposition time. Other than the Ti target current, which varied from coating to coating, the other deposition parameters remained constant for all of the coatings, i.e., total chamber pressure, 1.5×10^{-3} torr; substrate temperature, 200 °C; carbon target power, 2 kW; and bias voltage, −55 V. As shown in Table 1, a total of 10 different coatings were produced (T0-T9).

2.5 Observation and Analysis Equipment

The wear surfaces and cross sections of the coatings were observed using scanning electron microscopy (SEM) and x-ray mapping (energy dispersive spectrometer [EDS]). The elemental compositions of each coating were analyzed using glow discharge optical emission spectroscopy (GDOES).

3. Results

3.1 Coating Structure and Basic Mechanical Properties

3.1.1 Composition. Table 1 presents the Ti and C compositions of each a-C:$Ti_{x\%}$ coating. The $x\%$ value of the various coatings indicates the atomic percentage of Ti metal, and ranges from 0 to 51%. Table 1 shows that the coating thickness increases with increasing Ti concentration (i.e., with increasing titanium target current).

3.1.2 Microstructure. The microstructure of the a-C:$Ti_{x\%}$ coatings varies with the level of Ti addition. Figure 2(a) to (c) presents typical scanning electron photomicrographs of the

Table 1 Coating thickness, hardness, critical load, and elemental composition of current a-C:Ti$_{x\%}$ coatings

Case No.	Ti target current, A	Coating	Thickness, μm	Hardness, kgf/mm^2	Critical load, N	Elemental composition, at.%	
						Ti	C
T0	0	a:C-Ti$_{0\%}$	0.8	1268	100	0	100
T1	0.5	a:C-Ti$_{3\%}$	0.89	1180	100	3	97
T2	0.6	a:C-Ti$_{13\%}$	0.92	907	99	13	87
T3	1	a:C-Ti$_{20\%}$	1.2	866	99	20	80
T4	1.5	a:C-Ti$_{28\%}$	1.41	812	94	28	72
T5	2	a:C-Ti$_{35\%}$	1.44	950	99	35	65
T6	2.5	a:C-Ti$_{41\%}$	1.75	996	99	41	59
T7	3	a:C-Ti$_{43\%}$	1.96	1030	99	43	57
T8	3.5	a:C-Ti$_{49\%}$	1.98	1240	96	49	51
T9	4	a:C-Ti$_{51\%}$	2.0	1345	100	51	49

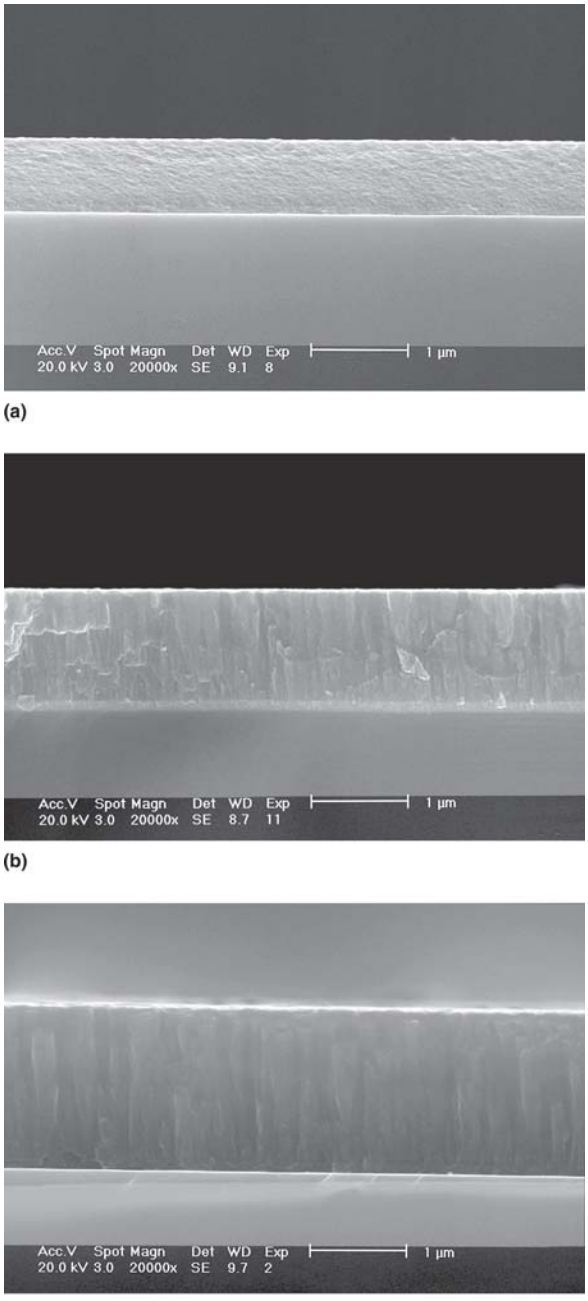

Fig. 2 Typical fracture cross sections of (a) a-C:Ti$_{3\%}$ (T1), (b) a-C:Ti$_{35\%}$ (T5), and (c) a-C:Ti$_{43\%}$ (T7) coatings

fracture cross sections of the a-C:Ti$_{3\%}$ (T1), a-C:Ti$_{35\%}$ (T5), and a-C:Ti$_{43\%}$ (T7) coatings, respectively. Figure 2(a) shows that the a-C:Ti$_{3\%}$ coating microstructure has a dense amorphous structure extending from the substrate to the coating surface. However, as Ti metal is added, a columnar structure is formed in the coating, as shown in Fig. 2(b). The columnar structure becomes increasingly pronounced as the level of Ti addition increases (Fig. 2c). As discussed in the following sections of this paper, the change in the coating microstructure induced by different levels of Ti addition causes a corresponding change in the mechanical properties, tribological behavior, and machining performance of the coatings.

3.1.3 Hardness. The hardness of each coating was measured using a nanoindentation tester (TriboScope, Hysitron Inc., Minneapolis, MN) with a force at final contact of 5 mN. The hardness values of the 10 coatings are summarized in Table 1. It is apparent that the coating hardness varies with the level of Ti addition. The coating hardness decreases as the Ti content is increased from 0 to 28 at.% (coatings T0-T4). However, the hardness then increases as the Ti content is further increased from 35 to 51 at.% (coatings T5-T9). Coatings T4 (a-C:Ti$_{28\%}$) and T9 (a-C:Ti$_{51\%}$) have the lowest and the highest hardness values, i.e., 812 and 1345 kgf/mm^2, respectively. Generally, harder materials have a higher wear resistance. Therefore, it is reasonable to assume that the a-C:Ti$_{51\%}$ coating will have an enhanced wear resistance. However, the tests performed later in this study reveal that the relationship between the coating's hardness and its wear resistance depends on the particular test performed, i.e., wear tests or machining tests. As will be shown later in Sections 3.2 and 3.3, the a-C:Ti$_{51\%}$ coating has a high friction coefficient and ultimately yields a poorer wear resistance than that of some of the other coatings.

3.1.4 Adhesion Characteristics. The adhesion characteristics of each coating were examined using a standard Rockwell-C hardness tester (ATK-F1000, Mitutoyo, Japan) under an applied load of 150 kgf. Arai et al. (Ref 23) observed the failure modes of thin films after indentation and proposed that the adhesion properties of a thin film can be estimated from the appearance (or absence) of radial and lateral cracks around the indentation. In the current study, the coatings displayed two basic failure modes, namely, plastic deformation or radial cracks around the indentation. Figure 3(a) (coating T3) shows the occurrence of plastic deformation around the indentation. This failure mode is generally indicative of coatings with good adhesion properties. Meanwhile, Fig. 3(b) shows the adhesion failure of the a-C:Ti$_{49\%}$ coating. In this case, radial cracks can be seen around the indentation, providing evidence of a poorer

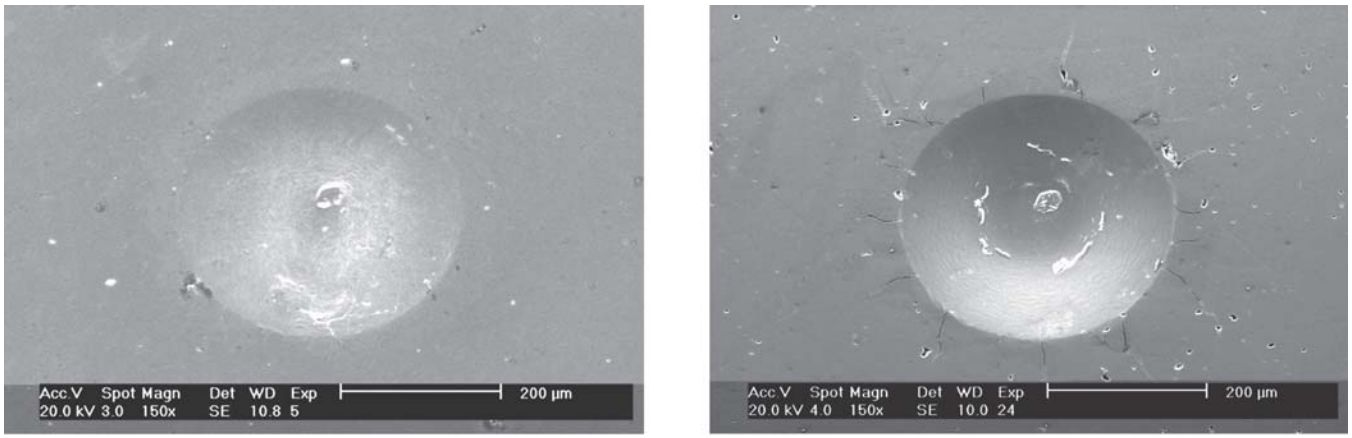

(a) (b)

Fig. 3 Typical failure modes of coatings after indentation: (a) a-C:$Ti_{20\%}$ (T3) and (b) a-C:$Ti_{49\%}$ (T8) coatings

Table 2 Wear results of a:C-$Ti_{x\%}$ coatings sliding against AISI 1045 steel wear pairs

Case No.	Coating	Wear test: Friction coefficient, 10 N f_a	10 N f_b	100 N f_a	100 N f_b	Wear depth *D*, µm: 10 N	100 N	Lifetime *L*, s: 10 N	100 N
T0	a:C-$Ti_{0\%}$	0.91	…	0.39	0.53	0.7	1.5	>1440	675
T1	a:C-$Ti_{3\%}$	0.64	…	0.18	0.83	0.1	0.6	>1440	1266
T2	a:C-$Ti_{13\%}$	0.37	…	0.12	0.91	0.4	0.8	>1440	1323
T3	a:C-$Ti_{20\%}$	0.55	…	0.20	0.50	0.6	0.9	>1440	1213
T4	a:C-$Ti_{28\%}$	0.80	…	0.29	1.13	0.7	2.3	>1440	559
T5	a:C-$Ti_{35\%}$	0.96	…	0.41	1.33	0.9	2.6	>1440	300
T6	a:C-$Ti_{41\%}$	1.22	2.08	0.43	1.17	1.4	3.3	855	83
T7	a:C-$Ti_{43\%}$	1.29	2.18	0.52	1.03	1.6	3.3	872	88
T8	a:C-$Ti_{49\%}$	1.21	1.69	0.51	1.35	1.7	2.7	653	33
T9	a:C-$Ti_{51\%}$	1.29	2.76	0.56	1.54	1.3	2.9	535	10
	Uncoated	…	2.82	…	0.95	0.7	3.2	…	…

Note: f_a, average value of low-friction coefficients during stable stage; f_b, average value of high-friction coefficients during fluctuating stage; *D*, wear depth of wear scar on coating; and L, lifetime of wear pairs under normal loadings of 10 and 100 N, respectively

coating adhesion. The failure modes of the a-C:$Ti_{0\%}$, a-C:$Ti_{3\%}$, and a-C:$Ti_{13\%}$ coatings all resemble that shown in Fig. 3(b). However, the adhesion characteristics of the coating improve as the titanium content increases. Therefore, the a-C:$Ti_{20\%}$, a-C:$Ti_{28\%}$, a-C:$Ti_{35\%}$, a-C:$Ti_{41\%}$, and a-C:$Ti_{43\%}$ coatings exhibit only plastic deformation around the indentation. Neither radial cracking nor annular detachment of the coating around the indentation is observed. This provides further evidence of the good adhesion characteristics of these particular coatings. However, the further addition of Ti leads to a reduction in adhesion. Hence, the failed a-C:$Ti_{49\%}$ and a-C:$Ti_{51\%}$ coatings both exhibit radial cracks around the indentation. The adhesive properties of the various coatings were also examined by performing scratch tests in which a 300 µm diameter diamond stylus was driven across each coating at a continuously increasing loading rate of 1 N s^{-1}. The nominal maximum load was specified as 100 N, and the critical load for each coating was defined as the load applied when the substrate first became visible at the base of the scratch track. As shown in Table 1, the scratch test results revealed that the coatings all possess high critical loads (>94 N). In other words, the current a-C:$Ti_{x\%}$ coatings all possess good adhesion properties. Furthermore, it is apparent that the adhesion strength is basically insensitive to the level of Ti metal addition.

3.2 Tribological Properties of Coatings Under Wear Testing

In the present wear tests, the friction coefficients of the wear pairs were continuously recorded under normal loads of 10 and 100 N, respectively. The resulting friction coefficient curves comprise two main regions. In the first region, the curve is smooth and corresponds to low-friction coefficients with an average value designated as f_a. In the second region, the curve fluctuates and corresponds to high friction coefficients with an average value of f_b. The lifetime (*L*) of the coating is defined as the duration of the first region, i.e., *L* represents the time from the start of testing until the time at which the friction coefficient suddenly increases and starts to fluctuate. Table 2 presents the wear depths and mean values of the friction coefficients of the current coatings obtained after wear testing for 24 min against an AISI 1045 steel counterbody. In this study, the tribological properties of each coating are classified as good, fair, or poor depending on the friction coefficient of the stable state (f_a), the wear depth, and the lifetime.

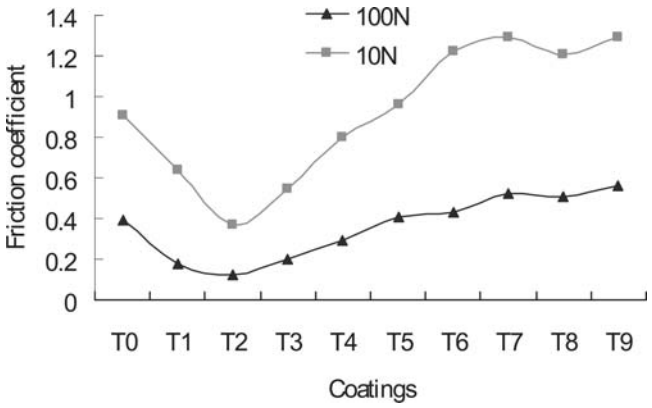

Fig. 4 Mean value of friction coefficient in the stable-state region under normal loadings of 10 and 100 N, respectively

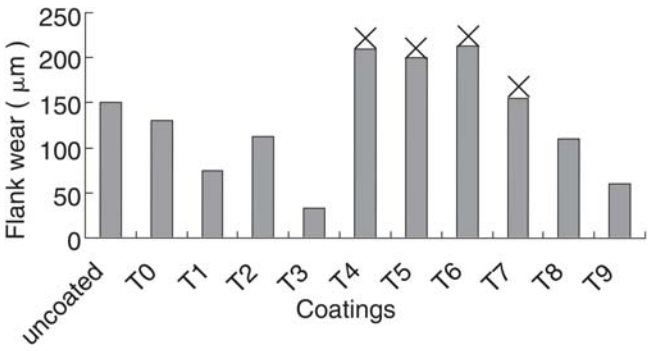

Fig. 5 Flank wear of turning cutters with different coatings after turning test. Note: Coatings marked with "×" failed before the turning test was completed. Hence, columns marked with "×" indicate flank wear of T4-, T6-, and T7-coated cutters measured after turning for 13.75 min and flank wear of T5-coated cutter measured after turning for 27.5 min.

Table 2 shows that coatings a-C:$Ti_{3\%}$, a-C:$Ti_{13\%}$, and a-C:$Ti_{20\%}$ (T1-T3) have good tribological properties, i.e., they have a low friction coefficient, a low wear depth, and a long lifetime under loadings of 10 and 100 N, respectively. The friction coefficients of these coatings vary between 0.37 and 0.64 (f_a) under a low loading of 10 N and their lifetimes exceed 1440 s. At a higher loading of 100 N, the friction coefficients fall significantly, i.e., f_a varies between 0.12 and 0.20, and a long lifetime is still achieved, i.e., between 1213 and 1323 s. Coatings T1-T3 also have good antiwear properties with wear depths ranging from 0.1 to 0.6 μm under a loading of 10 N and from 0.6 to 0.9 μm under a loading of 100 N. Referring to Table 1, it is clear that these wear depths are less than the coating thickness. Of these three coatings, the a-C:$Ti_{3\%}$ coating possesses the best antiwear properties (i.e., the lowest wear depth; 0.1 and 0.6 μm under loadings of 10 and 100 N, respectively), while the a-C:$Ti_{13\%}$ coating has the best antifriction properties (i.e., the lowest friction coefficient; $f_a = 0.37$ and $f_a = 0.12$ under loadings of 10 and 100 N, respectively). Table 2 shows that coatings T0, T4, and T5 (i.e., a-C:$Ti_{x\%}$ coatings with Ti additions of $x = 0\%$, 28%, and 35%, respectively) have a higher wear depth, i.e., between 0.7 and 0.9 μm under a loading of 10 N and between 1.5 and 2.6 μm under a loading of 100 N. These three coatings also have higher friction coefficients (f_a), i.e., between 0.8 and 0.96 under a loading of 10 N and between 0.29 and 0.41 under a loading of 100 N. For wear testing under a loading of 100 N, these coatings wear through to the substrate, and their lifetimes are reduced to less than 675 s. According to the classification presented above, these coatings demonstrate only fair tribological properties, and they are clearly unsuitable for sliding against a steel counterbody under a high normal load (100 N). Finally, coatings T6-T9 (i.e., a-C:$Ti_{x\%}$ coatings with Ti additions of $x = 41\%$, 43%, 49%, and 51%, respectively) exhibit the poorest tribological properties of all the current coatings under both low and high normal loads. Under a low load of 10 N, the wear scars on the coated disk have a depth of 1.3-1.7 μm and hence penetrate almost as far as the substrate. When a normal load of 100 N is applied, the wear depth ranges from 2.7 to 3.3 μm, and hence the wear scars actually penetrate the substrate. In addition, the friction coefficients of these four coatings range from high values of 1.22-1.29 (f_a) under a loading of 10 N to low values of 0.43-0.56 (f_a) under a loading of 100 N. Finally, the lifetimes of these coatings are all very short, particularly under a high normal load, i.e., $L < 88$ s.

Figure 4 shows that the friction coefficient (f_a) of the coating depends on the magnitude of the applied load and on the level of Ti metal addition. It is apparent that the friction coefficient decreases with increasing normal load. Furthermore, the friction coefficients of the coatings with a low Ti content (T1-T4) are lower than those of the high Ti content coatings (T5-T9) or that of the zero content coating (T0). The a-C:$Ti_{51\%}$ coating has the highest friction coefficient, indicating that it has very poor antifriction properties.

3.3 Machining Tests

3.3.1 Turning Performance. Figure 5 presents the experimental results obtained for the flank wear of each coating during the turning tests. It can be seen that the flank wear of the uncoated turning cutter (150 μm) is reduced in the coatings with Ti content <20% (coatings T0-T3) and >49% Ti content (coatings T8 and T9). Medium addition of Ti (i.e., coatings T4-T7) fails to improve the flank wear. In fact, these coated cutters fracture before the turning test is finished, as indicated by the "X" over the respective columns in Fig. 5. Coatings T4 (a-C:$Ti_{28\%}$), T6 (a-C:$Ti_{41\%}$), and T7 (a-C:$Ti_{43\%}$) fail after turning for 13.75 min. Coating T5 (a-C:$Ti_{35\%}$) fractures on the cutting edge and fails catastrophically after 27.5 min. Therefore, it is clear that coatings T4-T7 tend to shorten the service life of the cutters. Figure 6 shows the typical failure of the T6 coated cutter after fracture on the flank face. To investigate the fracture mechanism further, the T5 coated cutter was used in a two-stage cutting test in which the flank wear and cutting edge wear were measured after 13.75 min, and the flank wear was then measured after failure at 27.5 min. Figure 7(a) shows that the flank wear is comparatively mild after 13.75 min. However, Fig. 7(b) indicates that the cutting edge contains cracks and includes a significant volume of adherent workpiece material (AISI 1045 steel). After 27.5 min, the cutter breaks catastrophically, as shown in Fig. 7(c).

As shown in Fig. 5, the T3 and T9 coatings possess excellent flank wear resistance, i.e., these coatings improve the flank wear by an order of 4.5 and 2.5 times, respectively, compared with the uncoated cutter. Figure 8(a), to (c) and 7(c) show the typical flank wear morphology after the turning test of the

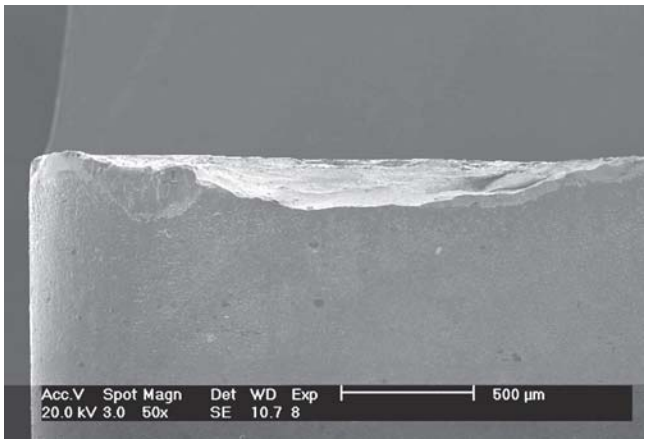

Fig. 6 Wear morphology of T6 (a:C-$Ti_{41\%}$) turning cutter after turning for 13.75 min

uncoated cutter and the T3-, T9-, and T5-coated cutters, respectively. Figure 8(a) shows that the flank face of the uncoated cutter suffers serious flank wear during testing, while Fig. 7(c) reveals that the T5-coated cutter fails completely. In other words, the T5 coating provides a totally inadequate wear protection for turning applications. Figure 8(b) and (c) shows that the T3 and T9 coatings reduce the flank wear considerably. In particular, the T3-coated cutter (Fig. 8b) has only mild flank wear, and only a small volume of work material adheres to the cutting edge.

3.3.2 Drilling Performance. To investigate the feasibility of applying the developed coatings for industrial machining applications, the a-C:$Ti_{x\%}$ coatings showing better flank wear resistance in the turning tests were selected for deposition on microdrills. Several drilling tests were then carried out using the coated drills. A comparative evaluation of the coating performance was performed by investigating the tool life in terms of the total attainable number of drilled holes before the corner wear value reached a value of 25 μm. Figure 9 shows the drilling test results for the corner wear of the uncoated microdrill and for the T3- and T9-coated microdrills. It is observed that the T9 coating consistently provides the optimal corner wear resistance. Specifically, the corner wear of this coated microdrill is approximately 2.3 times lower than that of the uncoated microdrill after the 20,000th hole has been drilled. Figure 9 also provides an indication of the tool lives of the two coated microdrills. The T3 coating increases the maximum attainable number of drilled holes from 1000 to 2600. Meanwhile, the T9 coating further increases the maximum number of attainable holes to 15,000.

4. Discussion

4.1 Transfer Layer Effect on Tribological Behavior

Figure 10 presents typical friction coefficient curves of the a-C:$Ti_{13\%}$ (T2) and a-C:$Ti_{43\%}$ (T7) coatings under loadings of 10 and 100 N, respectively. The a-C:$Ti_{13\%}$ coating has low friction coefficients and a smooth friction trace in the stable region under both loading conditions. Conversely, the a-C:$Ti_{43\%}$ coating has high friction coefficients and a significantly fluctuating trace under loadings of 10 and 100 N. The a-C:$Ti_{13\%}$ coating sliding against the AISI 1045 steel cylinder counterbody has a low and stable friction coefficient because a carbon-rich transfer layer is formed on the steel cylinder. The good tribological behavior between the coated disk and the protective film of the reciprocating sliding 1045 steel cylinder has a positive effect on the friction coefficient, wear resistance,

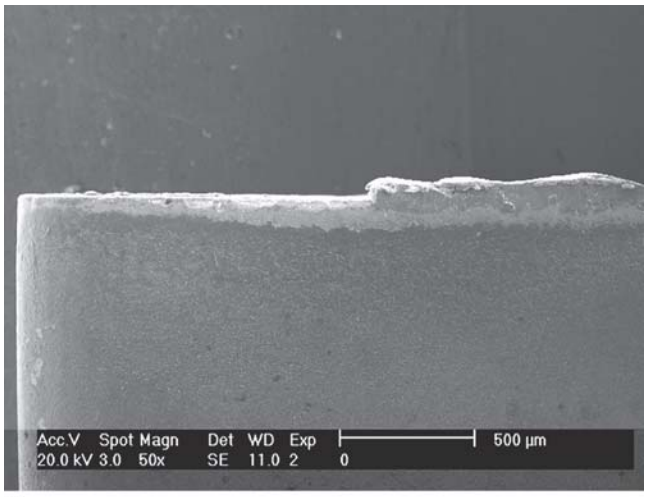

(a)

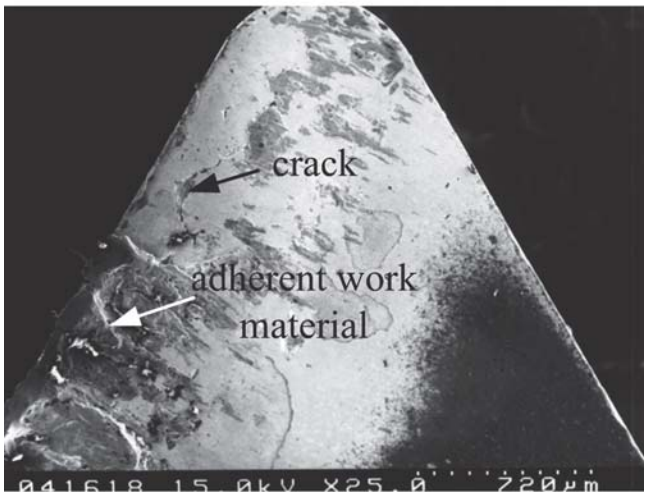

(b)

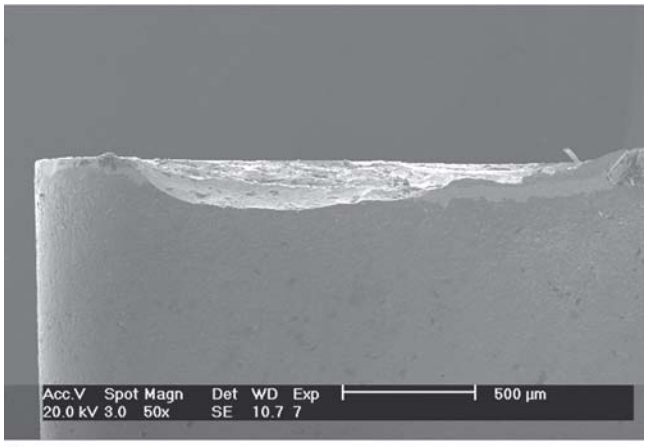

(c)

Fig. 7 Wear morphology of T5 (a-C:$Ti_{35\%}$) turning cutter: (a) flank wear and (b) cutting edge wear after testing for 13.75 min and (c) flank wear after testing for 27.5 min

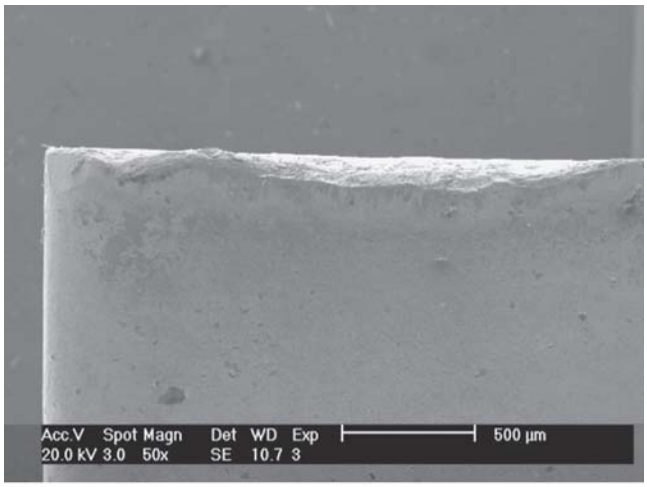

(a)

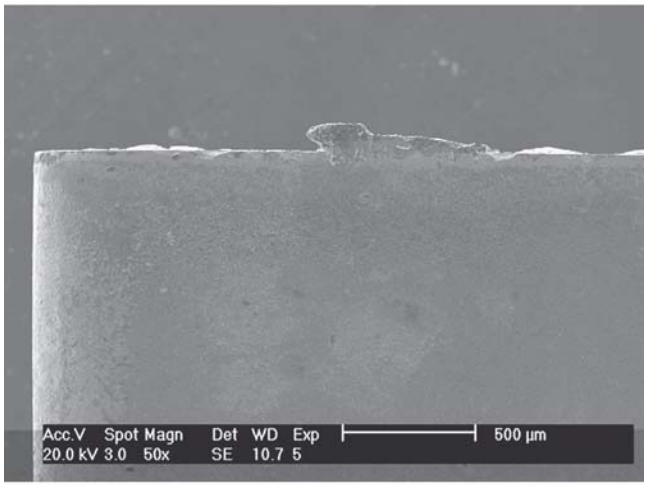

(b)

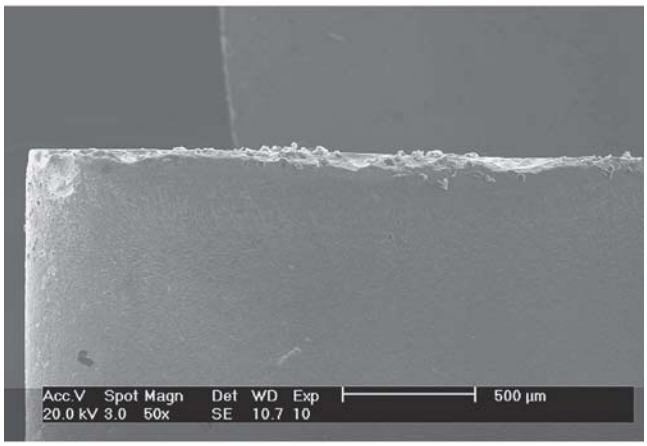

(c)

Fig. 8 Flank wear of turning cutters with different coatings after turning tests: (a) uncoated, (b) T3 (a-C:$Ti_{20\%}$), and (c) T9 (a-C:$Ti_{51\%}$)

and lifetime. Previous studies have reported that the formation of a thin transfer layer reduces wear and friction in DLC/counterbody wear pairs (Ref 24, 25). To examine the effect of the transfer layer on the tribological behaviors of the coatings with the best antiwear and antifriction properties, i.e., the a-C:$Ti_{3\%}$ and a-C:$Ti_{13\%}$ coatings, respectively, the transfer lay-

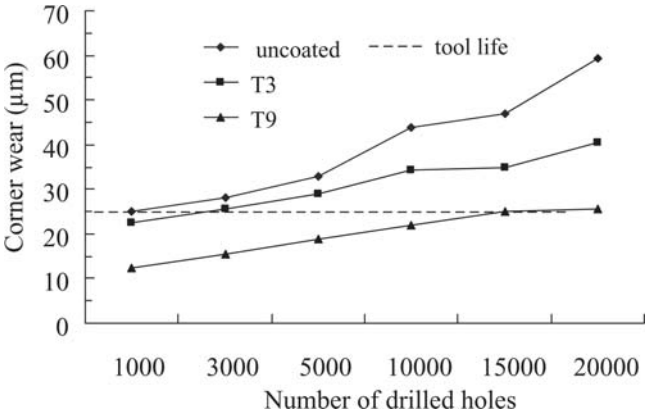

Fig. 9 Corner wear of uncoated and T3- (a-C:$Ti_{20\%}$) and T9-coated (a-C:$Ti_{51\%}$) microdrills as function of number of holes drilled

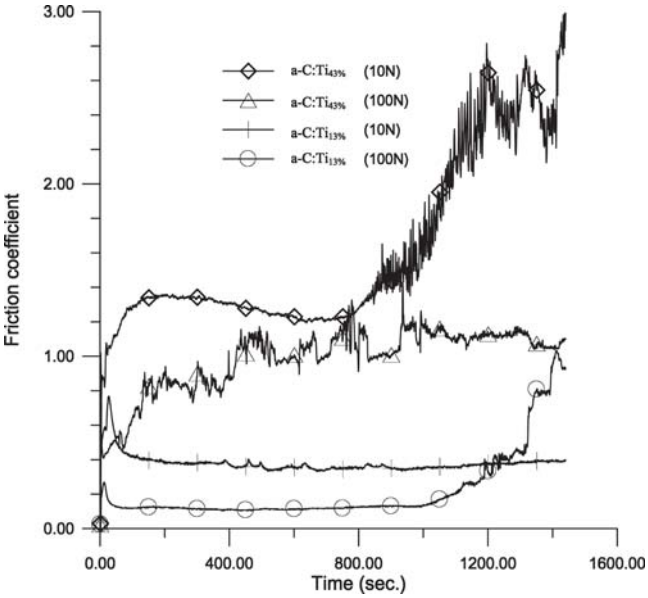

Fig. 10 Typical traces of friction coefficients of T2 (a-C:$Ti_{13\%}$) and T7 (a-C:$Ti_{43\%}$) coatings sliding against AISI 1045 steel counterbody under loadings of 10 and 100 N, respectively

ers formed on the wear scars of the AISI 1045 steel counterbody were observed during the wear stage corresponding to stable and low-friction coefficients. Figure 11(a) shows the a-C:$Ti_{3\%}$/1045-steel wear pair after testing for 600 s under a loading of 100 N. It is apparent that a patchy protective layer has been transferred from the a-C:$Ti_{3\%}$-coated disk to the AISI 1045 steel cylinder counterbody. Figure 11(b) presents a magnified photomicrograph of the region marked by the square in Fig. 11(a). The original machining marks on the 1045 steel cylinder are clearly visible beneath the transfer layer. Figure 11(c) presents the EDS analysis results for the wear scar shown in Fig. 11(b). It can be seen that both C and Ti are transferred from the a-C:$Ti_{3\%}$ coating to the counterbody. The transfer layer formed on the wear scar of the AISI 1045 steel cylinder improves the tribological properties by supplying a solid lubricant effect, thereby protecting the 1045 steel cylinder and the a-C:$Ti_{3\%}$ coating from serious damage. The wear on the AISI 1045 steel cylinder is found to be virtually zero, while the wear depth on the a-C:$Ti_{3\%}$ coating is the lowest of all the current

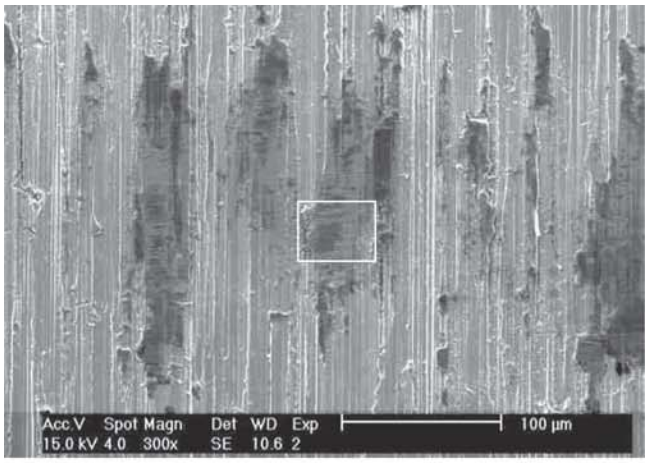

(a)

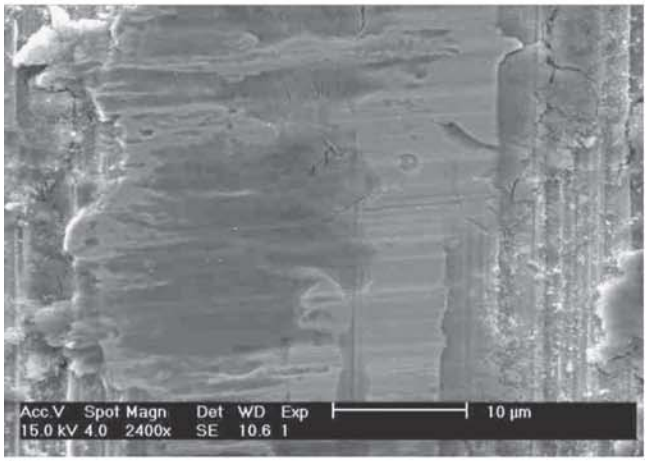

(b)

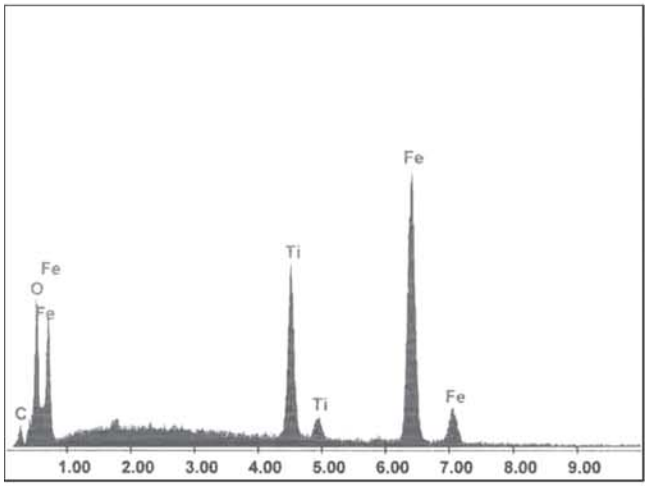

Element	Wt %	At %	K-Ratio	Z	A	F
C K	1.40	4.87	0.0039	1.1796	0.2332	1.0005
O K	10.33	26.97	0.0362	1.1565	0.3020	1.0021
TiK	17.37	15.14	0.1783	0.9770	0.9874	1.0641
FeK	70.90	53.01	0.6820	0.9725	0.9892	1.0000
Total	100.00	100.00				

(c)

Fig. 11 SEM photomicrographs of wear scars: (a) on AISI 1045 steel cylinder, (b) magnified photomicrograph of region marked "□" in (a), and (c) EDS analysis of wear scar shown in (b) for sliding against T1 (a-C:$Ti_{3\%}$) coating

coatings. Figure 12(a) shows the wear scar on the a-C:$Ti_{13\%}$/1045 steel wear pair after testing for 600 s under a loading of 100 N. Figure 12(b) presents a magnified photomicrograph of the area marked by the square in Fig. 12(a). In this case, a continuous transfer layer is formed on the wear scar on the 1045 steel. The EDS analysis corresponding to the wear scar in Fig. 12(b) shows a dramatic increase in the Ti/C peak compared with that shown in Fig. 11(c). Table 2 shows that the a-C:$Ti_{13\%}$ coating has the lowest friction coefficient, and the EDS results imply that a carbon-rich transfer layer is responsible for reducing the friction coefficient. A similar transfer layer is formed during the wear tests of the other a-C:$Ti_{x\%}$/1045 steel wear pairs. The transfer layer induces a low and stable friction coefficient. When the transfer layer fails, a high and fluctuating friction coefficient is generated, which causes serious damage to the coated disk (i.e., a higher wear depth). Coatings that provide longer lifetimes as a result of formation of a stable friction-reducing protective layer are characterized by a lower wear depth than the uncoated disk or the a-C:$Ti_{x\%}$/1045 steel wear pairs with a short lifetime.

4.2 Effect of Coating Properties on Machining Performance

The coating's adhesion strength, hardness, and tribological properties are the main factors that influence the turning results. The adhesion test results show that all of the a-C:$Ti_{x\%}$ coatings possess high adhesion strength (>94 N). Therefore, this property does not explain the difference in cutting performance observed for the different coated drills. Coatings T1, T2, and T3 possess good tribological properties, i.e., a low friction coefficient, a low wear depth, and a long lifetime, as shown in Table 2. The tribological properties of these coatings reduce the adhesion wear and therefore prevent a serious accumulation of adherent work material on the cutting edge (as shown in Fig. 8b). Consequently, these coatings reduce the flank wear of the cutter and increase its tool life. The T0, T8, and T9 coatings have a higher hardness than the other coatings. This property improves the wear resistance of the tool when an abrasive material rubs on its cutting edge. A typical cutter exhibits a uniform flank wear with some mild chipping (as shown in Fig. 8c). Coatings T4-T7 have poor tribological properties with lower hardness. This results in a more serious accumulation of adherent work material and leads to mechanical cracking (as shown in Fig. 7b). These coatings not only fail to improve the flank wear resistance but also lead to catastrophic fracture before the turning test is finished.

5. Conclusions

This study has shown that doping a-C:$Ti_{x\%}$ coatings with varying levels of Ti metal produces different microstructures, tribological properties, and machining performance. The microstructure of the a-C:$Ti_{x\%}$ coating is dense and amorphous at low levels of Ti addition but becomes increasingly columnar as the level of Ti addition is increased. The enhanced tribological properties obtained by doping the a-C:$Ti_{x\%}$ coatings with appropriate levels of Ti metal include a low friction coefficient, a low coating wear depth, and a long lifetime. The present results have demonstrated that the a-C:$Ti_{3\%}$ coating provides the best wear resistance properties, while the a-C:$Ti_{13\%}$ coating has the best antifriction characteristics.

In general, the present results show that good tribological

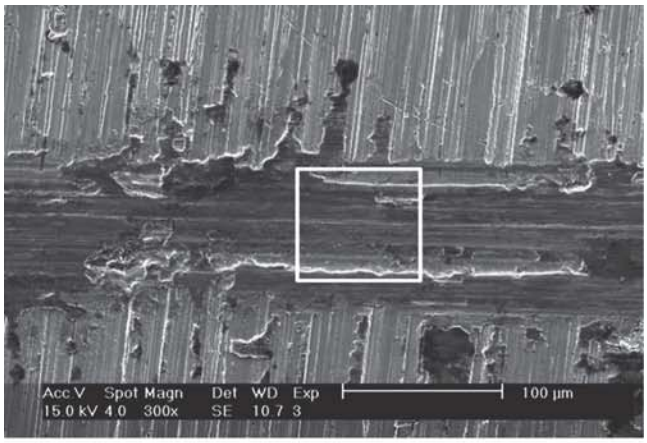

(a)

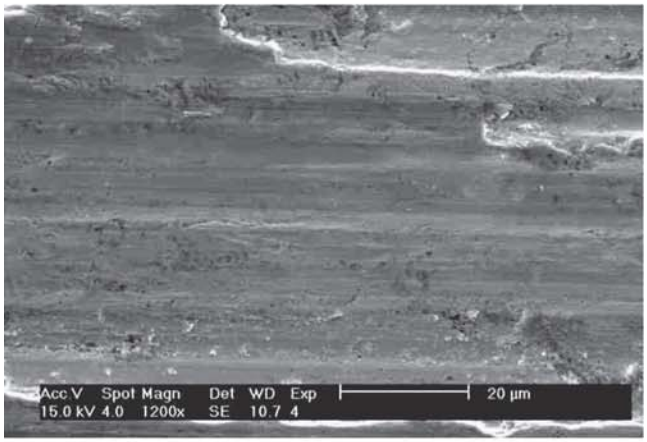

(b)

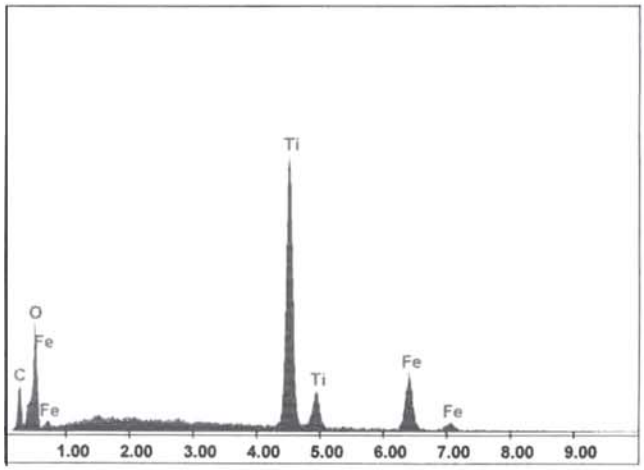

Element	Wt %	At %	K-Ratio	Z	A	F
C K	4.48	11.57	0.0159	1.1455	0.3106	1.0008
O K	22.27	43.20	0.0410	1.1233	0.1639	1.0004
TiK	49.02	31.76	0.4714	0.9461	0.9992	1.0174
FeK	24.24	13.47	0.2208	0.9399	0.9691	1.0000
Total	100.00	100.00				

(c)

Fig. 12 SEM photomicrographs of wear scars: (a) on AISI 1045 steel cylinder, (b) magnified photomicrograph of region marked "□" in (a), and (c) EDS analysis of wear scar shown in (b) for sliding against T2 (a-C:$Ti_{13\%}$) coating

properties and high hardness have the greatest effect on the turning performance of a coated tool. Coated cutters with good tribological properties and high hardness have enhanced adhesive wear resistance and abrasive wear resistance, respectively. Therefore, improving the machining performance of coated tools relies on fabricating coatings with high hardness and good tribological properties. However, the optimal Ti content depends on the specific application. For example, the present results have shown that coating cutters with a-C:$Ti_{20\%}$ and microdrills with a-C:$Ti_{51\%}$ increases the tool life by a factor of 4.5 and 15 times, respectively, compared with the uncoated tool case.

Acknowledgment

The authors thank the National Science Council of the Republic of China for financially supporting this research under contract no. NSC 93-2212-E-270-006-.

References

1. D. Liu, G. Benstetter, and E. Lodermeier, Surface Roughness, Mechanical and Tribological Properties of Ultrathin Tetrahedral Amorphous Carbon Coatings from Atomic Force Measurements, *Thin Solid Films,* 2003, **436,** p 244-249
2. P.W. Shum, Z.F. Zhou, and K.Y. Li, Tribological Performance of Amorphous Carbon Films Prepared on Steel Substrates with Carbon Implantation Pre-Treatment, *Wear,* 2004, **256,** p 362-373
3. P.W. Shum, Z.F. Zhou, and K.Y. Li, Optimisation of Carbon Implantation Pre-Treatments on the Adhesion Strength of Amorphous Carbon Coatings on AISI 440C Steel Substrates, *Surf. Coat. Technol.,* 2003, **166,** p 213-220
4. S. Zhang, X.L. Buia, X.T. Zeng, and X. Lic, Towards High Adherent and Tough a-C Coatings, *Thin Solid Films,* 2005, **482,** p 138-144
5. C. Charitidis and S. Logothetidis, Nanomechanical and Nanotribological Properties of Carbon Based Films, *Thin Solid Films,* 2005, **482,** p 120-125
6. H. Ronkainen, S. Varjus, J. Koskinen, and K. Holmberg, Differentiating the Tribological Performance of Hydrogenated and Hydrogen-Free DLC Coatings, *Wear,* 2000, **249,** p 260-266
7. V. Kulikovsky, P. Bohac, F. Franc, A. Deineka, V. Vorlicek, and L. Jastrabik, Hardness, Intrinsic Stress, and Structure of the a-C and a-C:H Films Prepared by Magnetron Sputtering, *Diamond Relat. Mater.,* 2001, **10,** p 1076-1081
8. G.A.J. Amaratunga, M. Chhowalla, C.J. Kiely, I. Alexandrou, R. Aharonov, and R.M. Devenish, Hard Elastic Carbon Films from Linking of Carbon Nanoparticles, *Nature,* 1996, **383,** p 321-323
9. J.C. Sanchez-Lopez, C. Donnet, J. Fontaine, M. Belin, A. Grill, V. Patel, and C. Jahnes, Diamond-Like Carbon Prepared by High Density Plasma, *Diamond Relat. Mater.,* 2000, **9,** p 638-642
10. M. Pancielejko, W. Precht, and A. Czyzniewski, Tribological Properties of PVD Titanium Carbides, *Vacuum,* 1999, **53,** p 57-60
11. A. Donnet and A. Grill, Friction Control of Diamond-Like Carbon Coatings, *Surf. Coat. Technol.,* 1997, **94-95,** p 456-462
12. T.L. Huu, H. Zaidi, and D. Paulmier, Lubricating Properties of Diamond-Like Coating, *Wear,* 1995, **181-183,** p 766-770
13. A. Erdemir, C. Bindal, J. Pagan, and P. Wilbur, Formation and Self-Lubricating Mechanisms of Boric Acid on Borided Steel Surfaces, *Surf. Coat. Technol.,* 1995, **76-77,** p 559-563
14. H. Fukui, J. Okida, N. Omori, H. Moriguchi, and K. Tsuda, Cutting Performance of DLC Coated Tools in Dry Machining Aluminum Alloys, *Surf. Coat. Technol.,* 2004, **187,** p 70-76
15. M. Rusop, T. Kinugawa, T. Soga, and T. Jimbo, Preparation and Microstructure Properties of Tetrahedral Amorphous Carbon Films by Pulsed Laser Deposition Using Camphoric Carbon Target, *Diamond Relat. Mater.,* 2004, **13,** p 2174-2179
16. W.I. Milne, J.T.H. Tsai, and K.B.K. Teo, Novel Field Emission Structure Based on Tetrahedrally Bonded Amorphous Carbon, *Diamond Relat. Mater.,* 2003, **12,** p 195-200
17. A.S. Loir, F. Garrelie, C. Donnet, J.L. Subtil, M. Belin, B. Forest, F. Rogemond, and P. Laporte, Mechanical and Tribological Characterization of Tetrahedral Diamond-Like Carbon Deposited by Femtosecond Pulsed Laser Deposition on Pre-Treated Orthopaedic Biomaterials, *Appl. Surf. Sci.,* 2005, **247,** p 225-231

18. R.J. Narayan, Laser Processing of Diamond-Like Carbon-Metal Composites, *Appl. Surf. Sci.,* 2005, **245,** p 420-430
19. V.N. Inkin, G.G. Kirpilenko, A.A. Dementjev, and K.I. Maslakov, A Superhard Diamond-Like Carbon Film, *Diamond Relat. Mater.,* 2000, **9,** p 715-721
20. S. Yang, D. Camino, A.H.S. Jones, and D.G. Teer, Deposition and Tribological Behaviour of Sputtered Carbon Hard Coatings, *Surf. Coat. Technol.,* 2000, **124,** p 110-116
21. D.Y. Wang, C.L. Chang, and W.Y. Ho, Characterization of Hydrogen-Free Diamond-Like Carbon Films Deposited by Pulsed Plasma Technology, *Thin Solid Films,* 1999, **355-356,** p 246-251
22. O.R. Monteiro and M.P. Delplancke-Ogletree, Investigation of Non-Hydrogenated DLC:Si Prepared by Cathodic Arc, *Surf. Coat. Technol.,* 2003, **163-164,** p 144-148
23. T. Arai, H. Fujita, and M. Watanabe, Evaluation of Adhesion Strength of Thin Hard Coatings, *Thin Solid Films,* 1987, **154,** p 387-401
24. H. Liu, A. Tanaka, and T. Kumagai, Influence of Sliding Mating Materials on the Tribological Behavior of Diamond-Like Carbon Films, *Thin Solid Films,* 1999, **352,** p 145-150
25. Y. Liu, A. Erdemir, and E.I. Meletis, A Study of the Wear Mechanism of Diamond-Like Carbon Films, *Surf. Coat. Technol.,* 1996, **82,** p 48-56